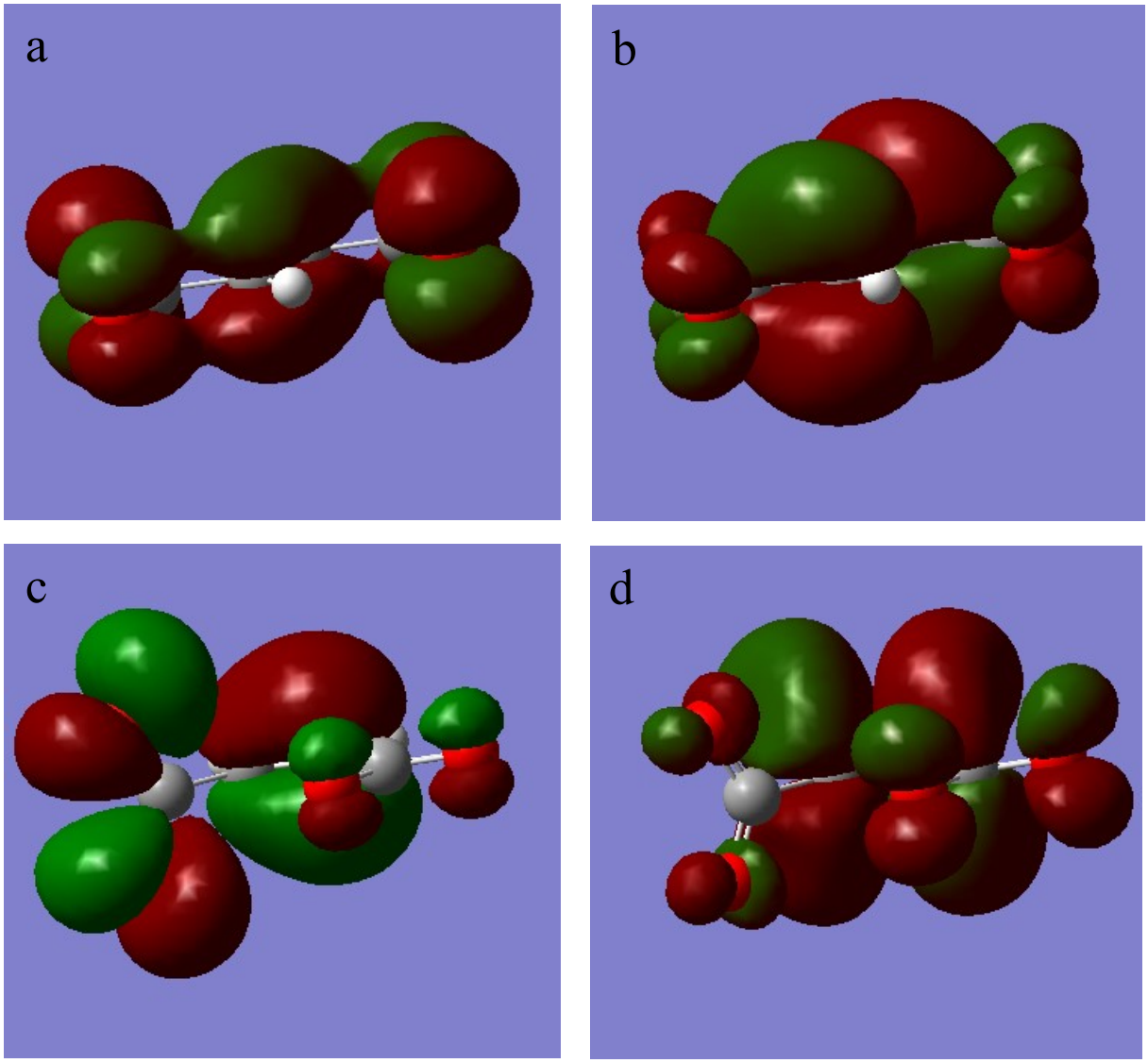

Fig. SI1 The natural transition orbitals for the $\pi \leftarrow \pi^*$ excitation of fumarate (a,b) and maleate (c,d).

1

2

3

4

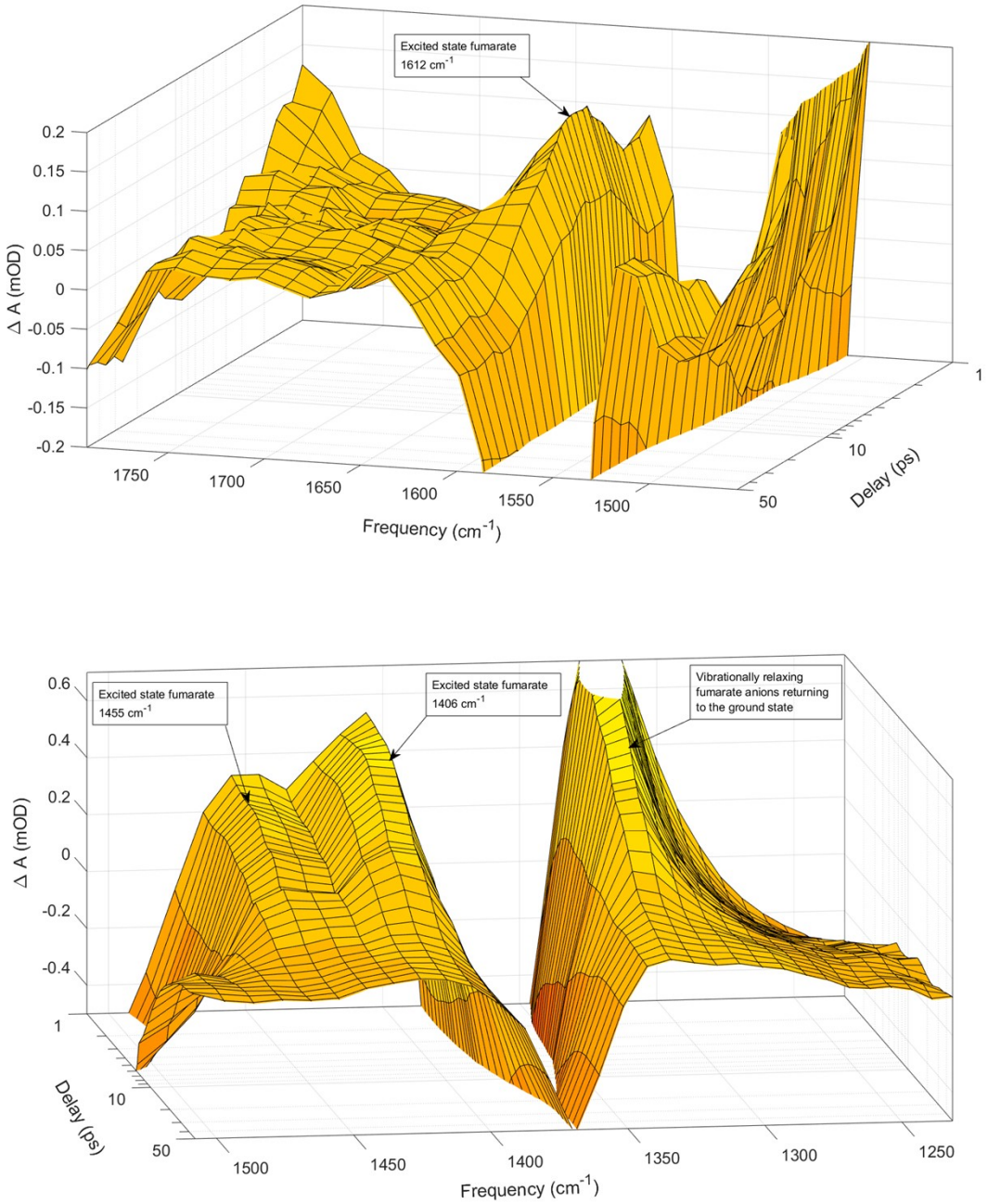

Fig. SI2. The transient absorption spectra of aqueous fumarate recorded as a function of time after the 200 nm excitation pulse. Here shown on a logarithmic timescale between 1ps and 50 ps. The lowest excited state of fumarate, ^1A_u, is identified by its 1406 cm^{-1}, 1455 cm^{-1} and 1612 cm^{-1} vibrational transitions observed at short delays. Also shown is the induced absorption associated with vibrationally relaxing fumarate anions returning to the ground state.

5

6

7

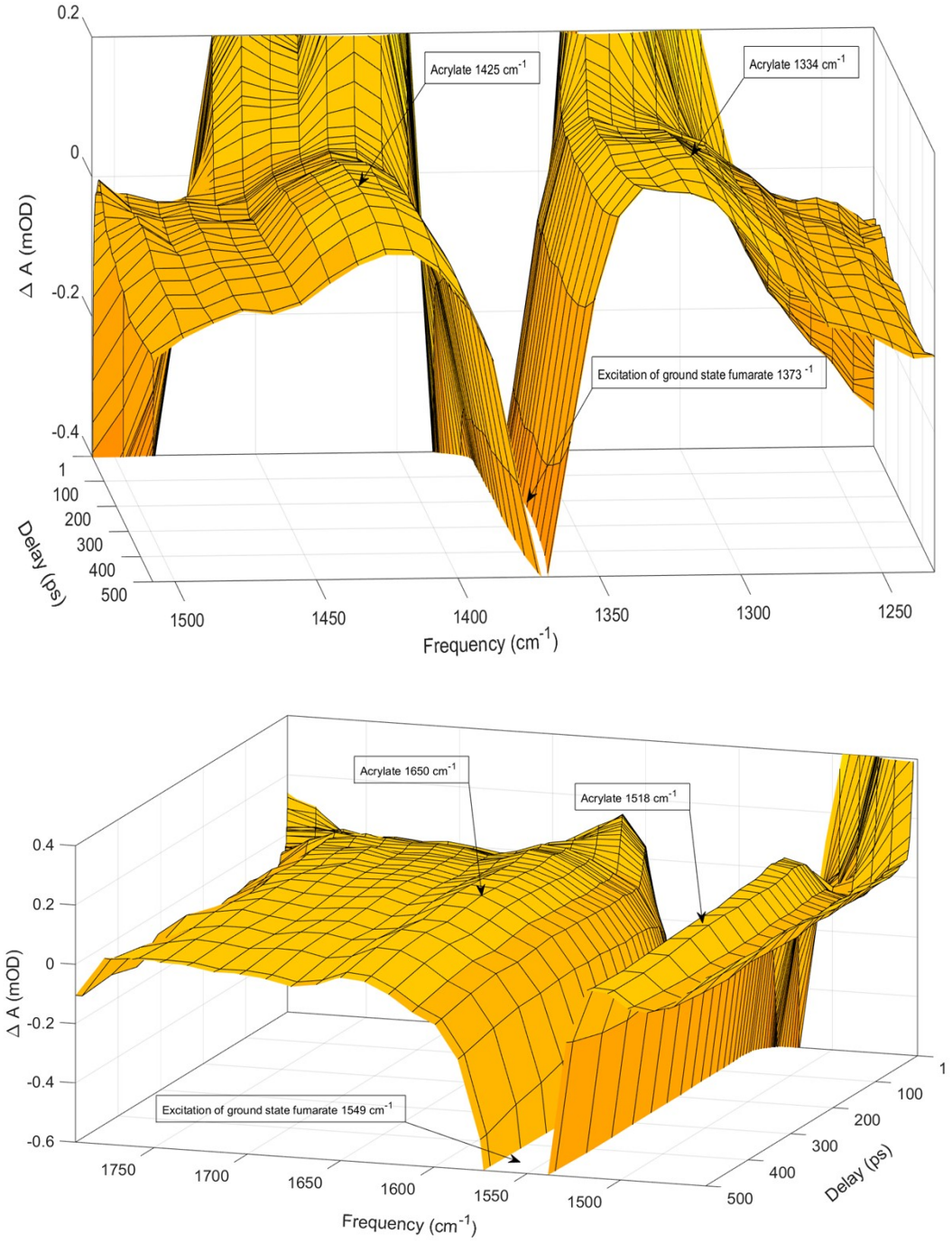

Fig. SI3. The transient absorption spectra of aqueous fumarate recorded as a function of time after the 200 nm excitation pulse. Here shown on a linear timescale between 1ps and 500 ps and with a truncated induced absorption axis. Acrylate is identified by the 1334 cm^{-1} and 1425 cm^{-1} transitions observed at long delays on either side of fumarate's symmetric carboxylate stretch at 1373 cm^{-1}. In addition, acrylate is identified by its asymmetric carboxylate stretch transition observed at 1518 cm^{-1} on the low frequency flank of the negative absorption pertaining to fumarate's asymmetric carboxylate stretch at 1549 cm^{-1}. Acrylate's transition expected at 1639 cm^{-1} shows up as the positive absorption around 1650 cm^{-1}.

8

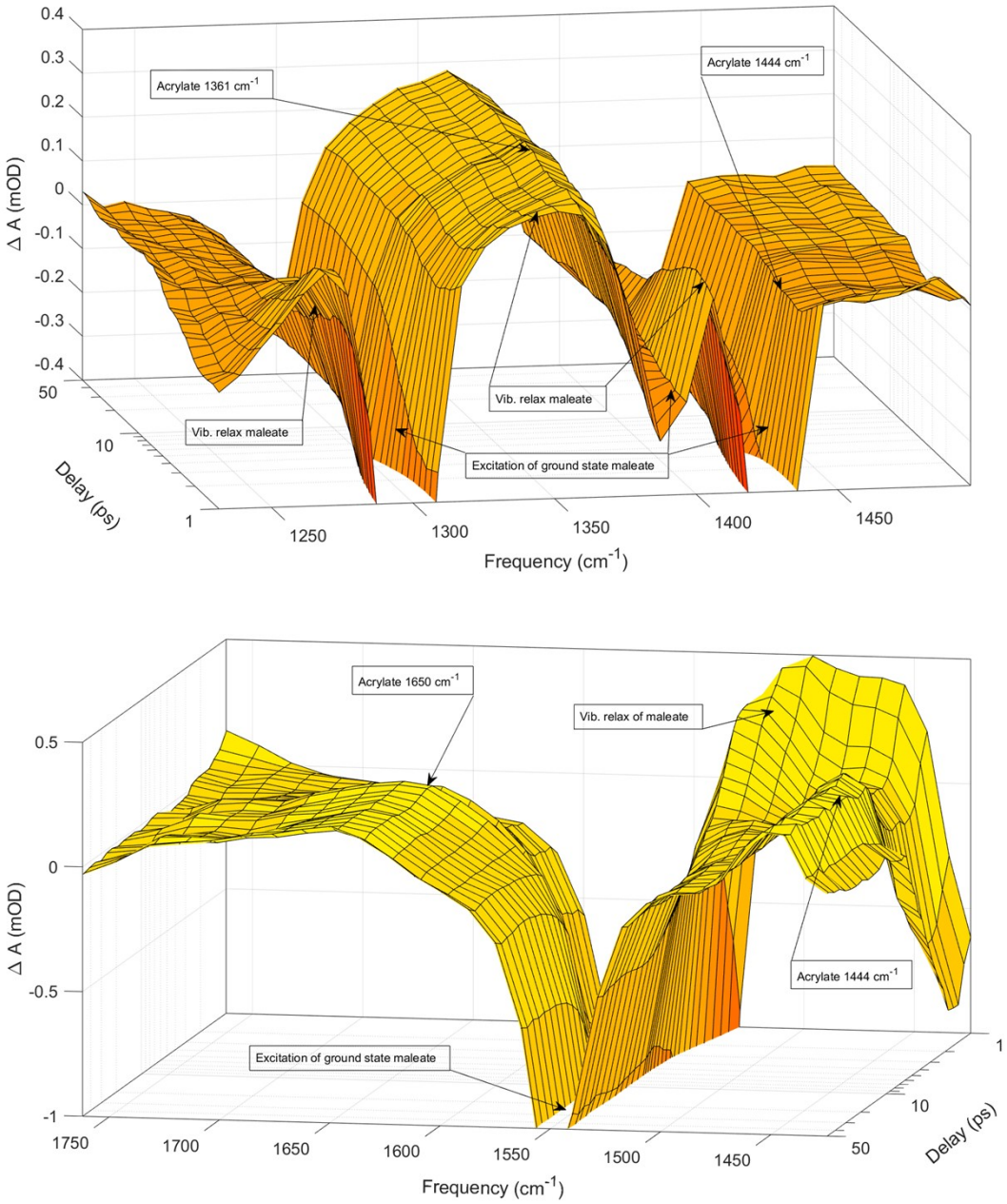

Fig. SI4. The transient absorption spectra of aqueous maleate recorded for the first 50 ps after the 200 nm excitation pulse. The spectra are shown on a logarithmic timescale with truncated induced absorption axis. Acrylate is identified by the positive absorption at 1361 cm^{-1}, 1444 cm^{-1} and 1650 cm^{-1}, while its transition at 1548 cm^{-1} is dominated by the negative absorption associated with the asymmetric carboxylate stretch of maleate. Acrylate appears 3 ps after the photoexcitation of maleate.

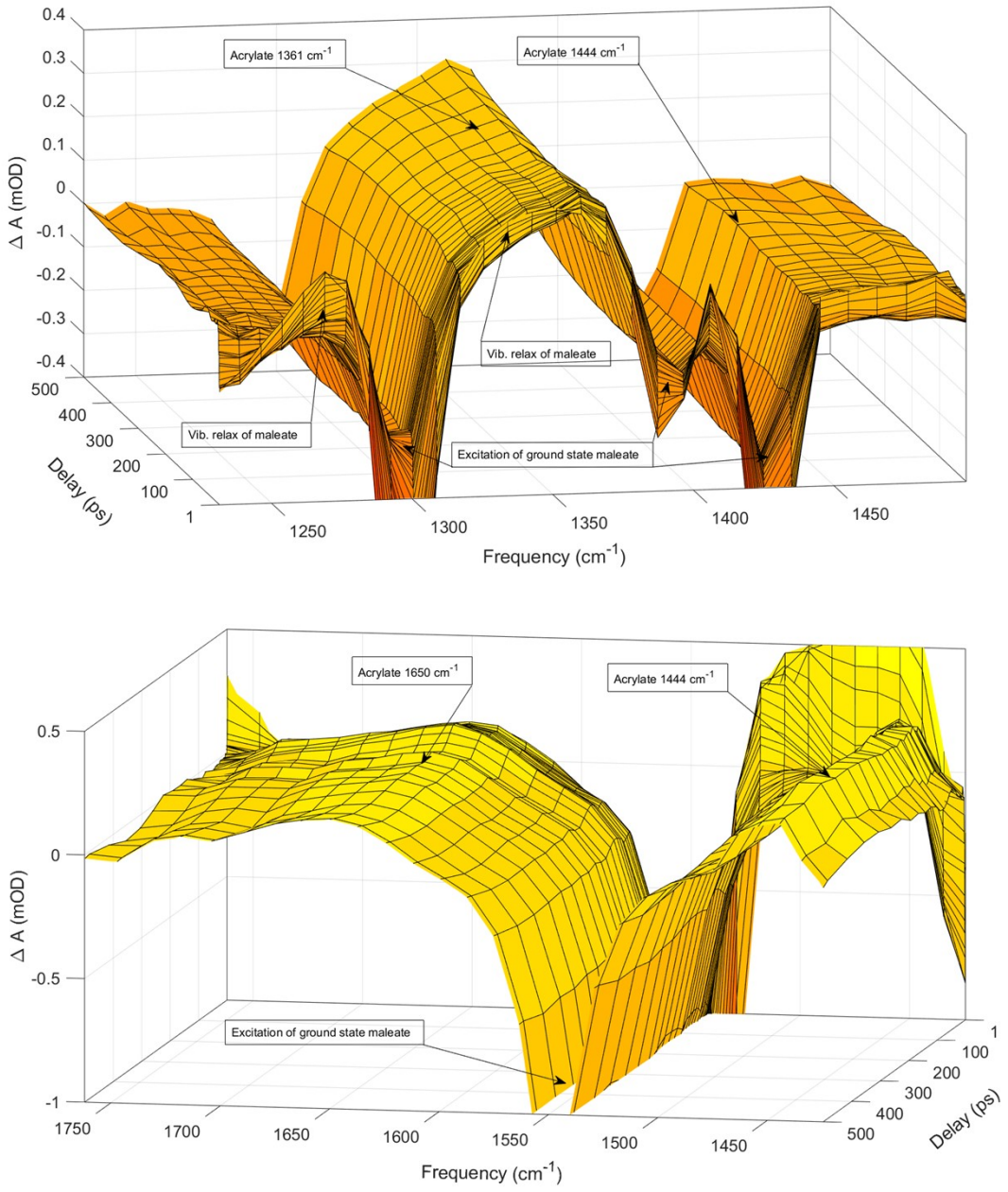

Fig. SI5. The transient absorption spectra of aqueous maleate recorded for the first 500 ps after the 200 nm excitation pulse. The data are shown on a linear timescale with truncated induced absorption axis. Acrylate is identified by the positive absorption at 1361 cm^{-1}, 1444 cm^{-1} and 1650 cm^{-1}, while its transition at 1548 cm^{-1} is dominated by the negative absorption associated with the asymmetric carboxylate stretch of maleate

9

10

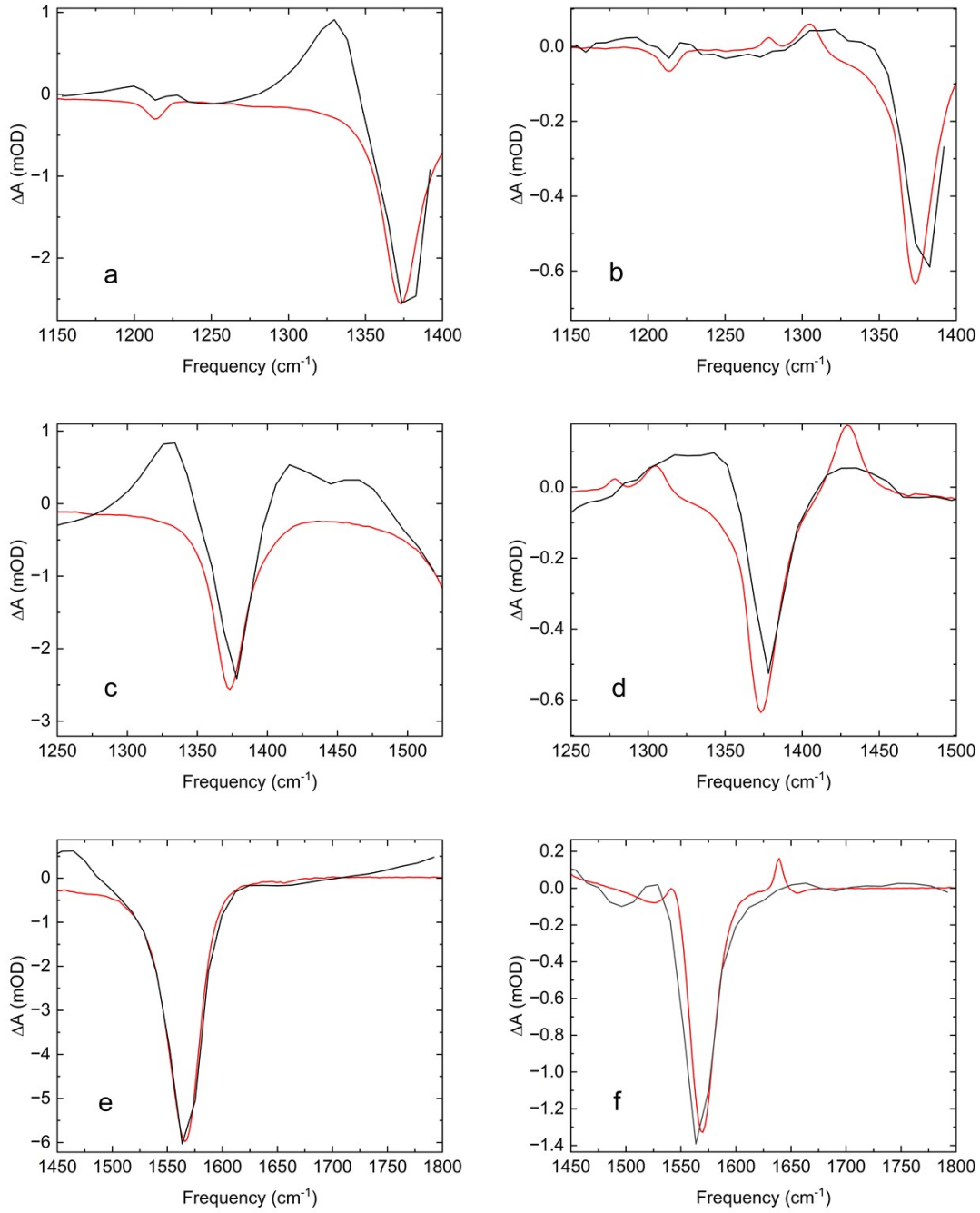

Fig. SI6 The figures (a), (c), and (e) compare the transient absorption recorded in fumarate after 1 ps (black curve) to the inverted steady state absorption spectrum of ground state fumarate (red curve). The figures (b), (d) and (f) compare the transient absorption after 100 ps (black curve) to the weighted sum of the inverted steady state absorption spectrum of ground state fumarate and the positive absorption from acrylate formed after decarboxylation of fumarate, in addition to maleate formed by isomerization of fumarate with yields of 20 % and 7%, respectively (red curve).

11

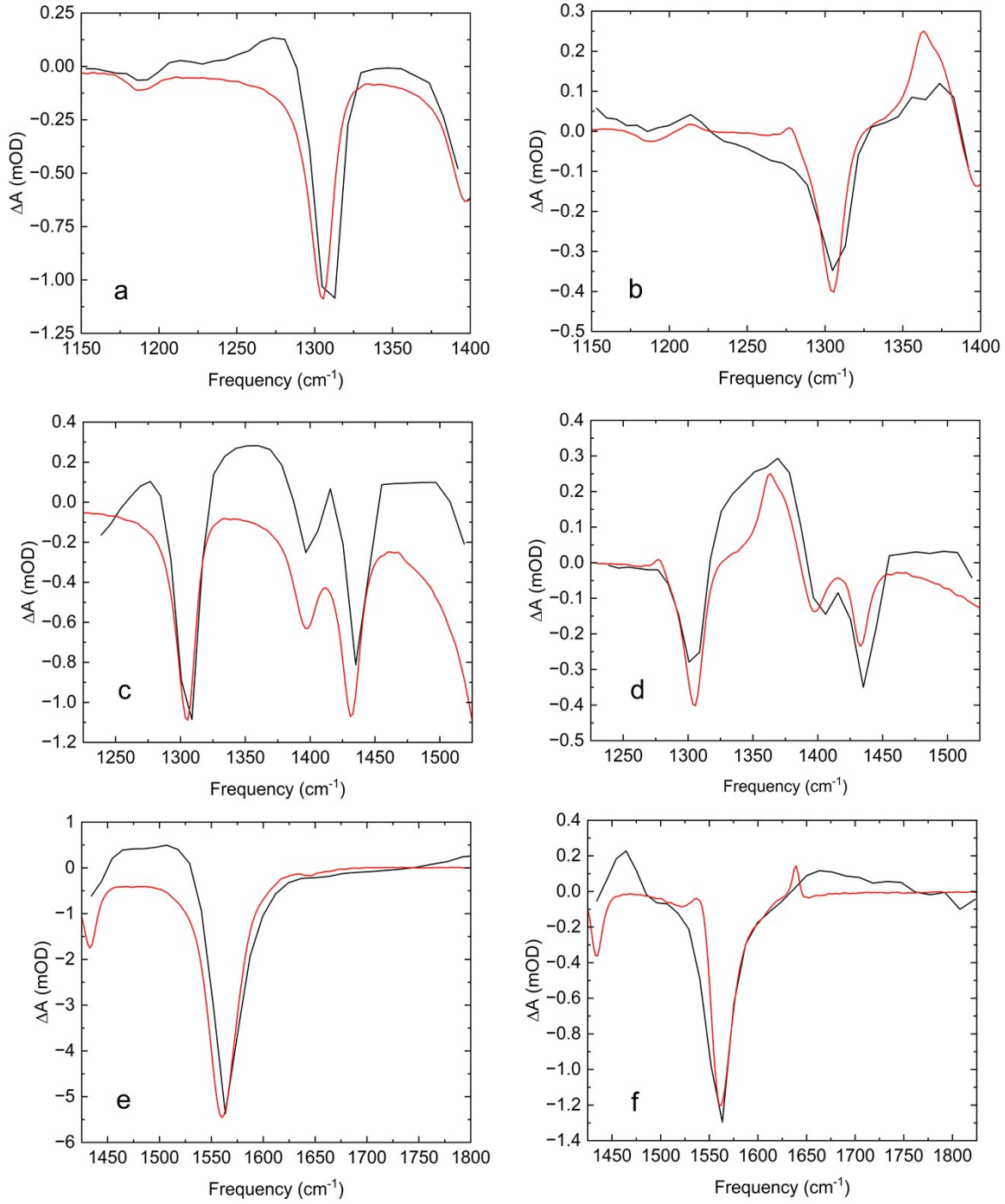

Fig. SI7. The figures (a), (c), and (e) compare the transient absorption recorded in maleate after 1 ps (black curve) to the inverted steady state absorption spectrum of ground state maleate (red curve). The figures (b), (d) and (f) compare the transient absorption after 100 ps (black curve) to the weighted sum of the inverted steady state absorption spectrum of ground state maleate and the positive absorption from acrylate formed after decarboxylation of maleate, in addition to fumarate formed by isomerization of maleate with yields of 20 % and 10%, respectively (red curve).

12

13

Table SI1 Calculated transition frequencies and intensities for ground state Fumarate + 4 D_2O compared to measured transition frequencies.

Vibration	Harm. Freq. (cm^{-1})	Anharm. Freq. (cm^{-1})	Harm. Int. (km/mol)	Anharm. Int. (km/mol)	Measured Freq. (cm^{-1})
out-of-plane CH bend	1020	1004	59	40	
asym. in-plane CH bend	1221	1071	14.2	35	1213
sym. in-plane CH bend	1296	1195	0	0	1276
asym. comb. sym. CO_2^-str.	1416	1390	1092	512	1373
sym. comb. sym. CO_2^-str.	1447	1420	0	0	
out-of-phase CO_2^- asym. str.	1620	1597	2	54	
in-phase CO_2^- asym. str.	1621	1591	1701	852	1558
C=C str.	1745	1696	0	0	1655

Table SI2 Calculated transition frequencies and intensities for ground state Maleate + 4 D_2O compared to measured transition frequencies.

Vibration	Harm. Freq. (cm^{-1})	Anharm. Freq. (cm^{-1})	Harm. Int. (km/mol)	Anharm. Int. (km/mol)	Measured Freq. (cm^{-1})
out-of-plane CH bend	1010	1001	1	1	
asym. in-plane CH bend	1214	1183	32	27	1186
sym. in-plane CH bend	1342	1314	214	49	1305
asym. comb. sym. CO_2^-str.	1445	1417	299	24	1396
sym. comb. sym. CO_2^-str.	1472	1442	328	247	1431
out-of-phase CO_2^- asym. str.	1615	1587	876	374	
in-phase CO_2^- asym. str.	1620	1597	946	275	1558
C=C str.	1732	1696	44	7	1655

Table SI3 Calculated transition frequencies and intensities for lowest excited state Fumarate ^1A_u + 6 D_2O compared to observed transient absorption frequencies.

Vibration	Harm. Freq. (cm^{-1})	Anharm. Freq. (cm^{-1})	Harm. Int. (km/mol)	Measured Freq. (cm^{-1})
C-C str.	1005	1041	7	
asym. in-plane CH bend	1188	1559	58	
sym. in-plane CH bend	1240	1135	103	
asym. CO_2^-str.	1287	1251	78	
sym. CO_2^-str.	1400	1359	1326	1406
sym. CO_2^-str.	1472	1491	1079	1455
asym. CO_2^-str.	1561	1571	1266	~1612
C=C str.	1715	1678	164	

Table SI4 Calculated transition frequencies and intensities for lowest excited state Maleate $^1A'$ + $6D_2O$.

Vibration	Harm. Freq. (cm^{-1})	Anharm. Freq. (cm^{-1})	Harm. Int. (km/mol)
sym. in-plane CH bend	1166	1114	141
comb. sym. CO_2^-str.+CH sym. bend	1258	1217	16
comb. asym. CO_2^-str.+ sym. CH bend	1375	1335	980
asym. comb. sym. CO_2^-str.+in-plane CH bend	1418	1384	40
sym. comb. asym CO_2^-str.+in-plane CH bend	1455	1407	561
asym. comb. asym. CO_2^-+in-plane CH bend	1489	1437	1892
C=C str.	1660	1602	136

Table SI5 Observed transients 100 ps after photodissociation of fumarate and the transition frequencies of acrylate measured by FTIR (Fig. 2(e) and (f)). Our calculations show that in the spectral region where we applied D_2O as solvent the spectral shift between the two isotopomers is less than 6 cm^{-1}.

Vibration	Acrylate Freq. (cm^{-1})	Observed Freq. (cm^{-1})
C-C str. + in-plane CH bend	1063	
in-plane CH bend	1279	
in-phase sym. str. CO_2^-sym. CH_2 bend	1361	~1334
out-of-phase sym. CO_2^-str.+ CH_2 in-plane bend	1431	1425
asym. CO_2^-str.	1548	~1518
C=C str.	1639	1650

Table SI6 Calculated transition frequencies and intensities for $^-HC{=}CHCO_2^-$ + 2 D_2O

Harm. Freq. (cm^{-1})	Anharm. Freq. (cm^{-1})	Harm. Int. (km/mol)	Anharm. Int. (km/mol)
1060	1325	48	63
1130	1686	3	27
1306	1390	36	36
1404	1363	690	522
1534	1506	503	586
1584	1562	360	68

Table SI7 Calculated transition frequencies and intensities for $^{\bullet}HC{=}CHCO_2^-$ + 2 D_2O

Harm. Freq. (cm^{-1})	Anharm. Freq. (cm^{-1})	Harm. Int. (km/mol)	Anharm. Int. (km/mol)
1206	1158	41	23
1391	1363	547	368
1634	1595	722	65
1676	1645	166	439

Table SI8
Lowest triplet excited state + 2 D_2O common to fumarate and maleate.

Harm. Freq. (cm^{-1})	Anharm. Freq. (cm^{-1})	Harm. Int. (km/mol)
1115	1206	4
1239	1273	273
1362	1347	23
1388	1370	762
1419	1390	340
1586	1571	1861
1589	1572	282

Table SI9 Observed transients 100 ps after photodissociation of maleate and the measured transition frequencies of acrylate measured by FTIR (Fig. 2(e) and (f)). Our calculations show that in the spectral region where we applied D_2O as solvent the spectral shift between the two isotopomers is less than 6 cm^{-1}.

Vibration	Acrylate Freq. (cm^{-1})	Observed Freq. (cm^{-1})
C-C str. + in-plane CH bend	1063	
in-plane CH bend	1279	
in-phase sym. str. CO_2^- sym. CH_2 bend	1361	~1361
out-of-phase sym. CO_2^- str.+ CH_2 in-plane bend	1431	1444
asym. CO_2^- str.	1548	
C=C str.	1639	1650